Phase diagrams and multicritical points in randomly mixed magnets. III. Competing spin-glass and magnetic ordering

Shmuel Fishman* and Amnon Aharony†
Department of Physics and Astronomy, Tel Aviv University, Ramat Aviv, Israel
(Received 12 March 1979)

The phase diagrams and critical properties of a quenched random alloy of a ferromagnet and an antiferromagnet (or of two antiferromagnets with different periodicities) are studied in the mean-field approximation and by renormalization-group techniques in $d = 6 - \epsilon$ dimensions, using the $n \to 0$ replica method. If only nearest-neighbor interactions are assumed, then one finds ferromagnetic (F), antiferromagnetic (AF), and spin-glass (SG) phases. As the average strength of the next-nearest-neighbor interactions is increased (e.g., by an additional component in the alloy), the F and the AF phases approach each other, and one may find regions in parameter space where a mixed F-AF phase exists, as discussed in Paper II of this series. The phase diagram exhibits lines of multicritical points where the paramagnetic (P), F (or AF) and SG phases coexist (P-SG-F or P-SG-AF), or where the P, F, and AF phases coexist (P-F-AF). These lines meet at a new multicritical point, where all four phases coexist (P-SG-F-AF). Recent renormalization-group analysis of P-SG-F, by Chen and Lubensky, yields complex exponents for the XY and Heisenberg cases. We show that the phase diagram predicted by that analysis is difficult to understand even for the Ising case. The same method of analysis yields similar difficulties for P-SG-F-AF. A modified way to take the limit $n \to 0$, which resolves these difficulties, is presented. This modified way still lacks rigorous justification.

I. INTRODUCTION

In the present series of papers we study the p-T (relative-concentration–temperature) phase diagrams of quenched random alloys prepared by mixing materials that exhibit different magnetic properties. In the first paper of this series[1] (denoted I) we studied a random alloy consisting of materials with competing anisotropies. In that case we found that in addition to the ordered phases which occur in the two components when they are pure, the alloy also exhibits a "mixed" phase, in which the order parameters of these two phases coexist. We found that these three ordered phases and the paramagnetic phase all coexist at a *decoupled tetracritical point.* In the second paper of this series[2] (denoted II) we studied a random alloy consisting of two magnetic materials which show (when pure) magnetic orderings with different periodicities, e.g., ferromagnetic (F) and antiferromagnetic (AF) (or different antiferromagnetic) phases. A mean-field-theory (MFT) analysis of this case, described in II, gave the phase diagrams shown in Fig. 1. The tetracritical point [Fig. 1(a)] or bicritical point [Fig. 1(b)] results when next-nearest-neighbor interactions are introduced. With only nearest-neighbor (NN) interactions, this multicritical point (and the mixed phase) does not exist at any finite temperature, and the phase diagram of Fig. 1(c) may result.[2] (MFT gives $p_F = p_A$ at this point, but fluctuations and frustration effects may yield a finite concentration range $p_F < p < p_A$ where the paramagnetic phase extends down to zero temperature.)

Competition between positive (ferromagnetic) and negative (antiferromagnetic) exchange interactions has been recently considered to be responsible for a new type of magnetic ordering, i.e., that of a spin-glass (SG).[3] Although this phase has been experimentally observed mainly in metallic alloys, charac-

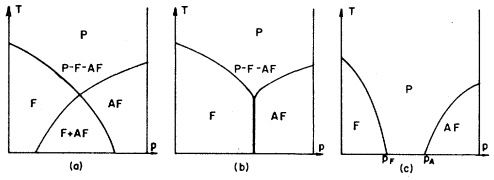

FIG. 1. Schematic sections of the phase diagrams of random alloys mixing an antiferromagnetic, (with concentration p) with a ferromagnet, without spin-glass ordering. P, F, and AF are the paramagnetic, ferromagnetic and antiferromagnetic phases. A bold line denotes a first order transition. (a) Tetracritical point and mixed phase. (b) Bicritical point. (c) The paramagnetic phase exists down to zero temperature.

terized by long-range Ruderman-Kittel-Kasuya-Yosida (RKKY) interactions,[4,5] it has been recently shown (by computer experiments) to also exist for competing positive and negative NN interactions.[6,7] In recent publications,[8,9] Harris, Lubensky and Chen suggested that Fig. 1(c) may in some cases be replaced by the phase diagram shown in Fig. 2(a).

If we do not confine ourselves to NN interactions, then in principle all the diagrams of Figs. 1,2, and possibly combinations of them may occur. In particular, alloys in which two concentrations (p_1 and p_2) can be varied experimentally could in principle yield a multicritical point at which the F, AF and SG order parameters all become critical simultaneously. Viewed from the paramagnetic phase, the phase diagram in the p_1-p_2 plane could assume the form shown in Fig. 2(b). In this work we study the conditions under which each of these phase diagrams is obtained.

We shall assume that the interactions are short ranged, as is usually the case in insulating magnetic materials. The MFT results of Figs. 1 and 2 describe the phase diagrams quantitatively only at sufficiently high dimensionalities, i.e., $d > 4$ for Fig. 1[2] and $d > 6$ for Fig. 2.[8,9] Below these dimensionalities the effects of critical fluctuations may be introduced using renormalization-group (RG) theory. When this was done for the multicritical point P-F-AF of Figs. 1(a) and 1(b) no stable fixed point was found.[2] Therefore, the nature of the transitions near P-F-AF may be significantly changed by fluctuations. One of the possibilities we raised in II was the allowance for a SG ordering. This is one of the motivations for the present study.

In I and II the results were the same for bond and site randomness, since the order parameters were *average* magnetizations, ignoring the identity of the magnetic ion at each site. When a SG order parameter is introduced in an alloy with NN interactions only, special types of site randomness are known to lead to different SG orderings.[10,11] We shall confine ourselves to *bond* randomness leading to the SG ordering usually characterized by the Edwards-Anderson (EA)[3] order parameter, $q = [\langle \vec{S}_i \rangle^2]_{av}$ (the average is over the random configurations). This was the order parameter used by Chen and Lubensky[9] to obtain the phase diagram of Fig. 2(a). Serious doubts were recently raised concerning the relevance of the EA order parameter in realistic dimensionalities. High-temperature expansions[12] indicate that the EA order parameter vanishes at $d = 4$ since the Ising-model SG susceptibility exponent γ_Q diverges as $d \to 4^+$. Real-space RG calculations for the Ising model with NN interactions indicate existence of a SG phase at 3 dimensions[13,14] and some calculations show SG ordering even in 2 dimensions.[14,15] Real-space calculations do not identify the order parameter appropriate for the description of the ordered phase, and therefore the SG they predict is not necessarily that described by the EA order parameter. Computer simulations for the Ising model with NN interactions only show controversial results (some of them show that the SG is a stable thermodynamic phase[6,7] and others indicate that the SG ordering decays after a long time).[16] It is possible that SG ordering exists for $d < 4$ but is not described by the EA order parameter. It is possible that the SG is not a thermodynamically stable phase, but is a phase where correlations decay much slower than exponentially. In this work we confine ourselves to the vicinity of the transitions from the paramagnetic phase, since we work in the framework of the Landau-Ginzburg-Wilson Hamiltonian. In this region use of the the EA order parameter gives correct results in the Sherrington-Kirkpatrick (SK) long-ranged model,[17] compared to computer simulations and to the modified MFT of Thouless, Anderson, and Palmer.[18] It is assumed that the results will be qualitatively correct also in the short-ranged model studied in the present work. This assumption is encouraged by a recent calculation by Klein *et al.*,[19] which shows that (for a Gaussian distributed exchange model) the phase diagram changes very little as the coordination number z is varied for $z \geq 8$.

We shall use the "$n \to 0$ replica method"[3] in order to obtain (in Sec. II and Appendix A) an effective Hamiltonian by a Hubbard[20] transformation in a way similar to that of SK.[17] A serious difficulty arises in the MFT analysis when the "$n \to 0$ method" is applied, since the free energy extremum is not a minimum in the SG phase in the limit $n \to 0$.[8,9,17] However, if the minimization procedure is done for $n \geq 2$ then it yields correct results for the SK model,[17] and therefore the same procedure will also be adopted here. A detailed discussion of this point is given in Sec. III below. In Sec. IV, RG theory in $d = 6 - \epsilon$ dimensions is applied to study the critical properties of the random alloys in various regions of

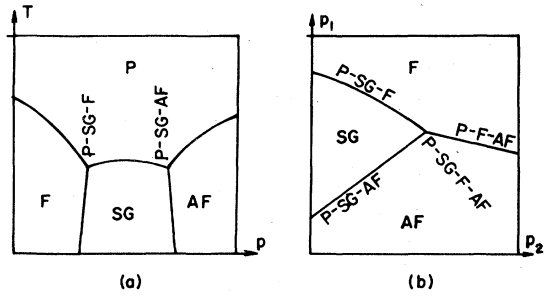

FIG. 2. Schematic sections of the phase diagrams when spin-glass (SG) ordering is introduced. (a) Concentration-temperature diagram, exhibiting an intermediate spin-glass phase. (b) View from the paramagnetic phase of the various ordered phases and multicritical lines.

the phase diagram (Figs. 1 and 2). For the boundaries between the F and AF phases with the paramagnetic phase P, and for the multicritical points where F, AF, and P coexist (P-F-AF), the critical dimensionality is $d_c=4$, and therefore MFT applies in $6-\epsilon>4$ dimensions (the critical properties in $4-\epsilon$ dimensions were studied in II). For the transition from the paramagnetic to the SG phase, the analysis of Ref. 8 applies. In Sec. IV, we calculate the critical properties of the multicritical points (MCP); (a) where the P, SG, and F (or AF) phases coexist (P-SG-F or P-SG-AF), and (b) where the P, SG, F, and AF phases all coexist (P-SG-F-AF). The critical properties of P-SG-AF are identical to those of P-SG-F, and should not be analyzed separately. Chen and Lubensky[9] studied the critical properties of P-SG-F, using an $\epsilon=6-d$ expansion ($d_c=6$). They found complex critical exponents for the Heisenberg ($m=3$) and XY ($m=2$) cases, a result which is difficult to understand, leading for instance to a situation where for a range of concentrations the ordered phase is the high-temperature phase. In Secs. IV and V we discuss this problem in detail. In particular we show that the results of Ref. 9 lead to problems in the structure of the phase diagram even for the Ising ($m=1$) case. We then present a modified way to take the limit $n\to 0$, in which these problems are eliminated. The physical interpretation of the RG results in terms of scaling fields and phase diagrams is given in Sec. V. Finally, the results are discussed in Sec. VI.

II. HAMILTONIAN

Our initial Hamiltonian is identical to that discussed in Paper II: we start with m-component spins $\vec{\sigma}(i)$ on a d-dimensional lattice, with random exchange coefficients J_{ij},

$$\mathcal{H}\{J_{ij},\vec{\sigma}(i)\}=-\tfrac{1}{2}\sum_{i\neq j}J_{ij}\vec{\sigma}(i)\cdot\vec{\sigma}(j)\ . \tag{2.1}$$

We next assume a magnetic unit cell of $l=2^L$ spins, and define cell spin variables

$$\vec{\phi}_k(j)=\sum_{p=1}^{l}F_{kp}\vec{\sigma}(p,j)\ , \tag{2.2}$$

where j runs over cells, p runs over spins in the cell, k runs over types of magnetic ground-state ordering, and F is an orthogonal matrix, the elements of which can be chosen to be $F_{kp}=\pm 1/\sqrt{l}$.

We now use the "replica method",[3,21] replacing $\vec{\phi}_k$ by $\{\vec{\phi}_k^{\,\alpha},\ \alpha=1,2,\ldots,n\}$ and averaging over the random values of the new coefficients

$$J_{ij}^{kk'}=\sum_{p,p'=1}^{l}J_{ip,jp'}F_{kp}F_{k'p'}\ . \tag{2.3}$$

A cumulant expansion, using the fact that $\mathcal{H}$ must be an even function of the $\vec{\phi}_k^{\,\alpha}$'s for each k separately, then yields the effective Hamiltonian (see Paper II)

$$\begin{aligned}\mathcal{H}_{\rm eff}=&-\tfrac{1}{2}\sum_{j,i}\sum_{k=1}^{l}[J_{ij}^{kk}]_{\rm av}\sum_{\alpha=1}^{n}\vec{\phi}_k^{\,\alpha}(i)\cdot\vec{\phi}_k^{\,\alpha}(j)\\&-\tfrac{1}{2}\sum_{j,i}\sum_{k,k'}\Bigg[(\Delta_{ij}/k_BTl^2)\sum_{\alpha,\beta}\vec{\phi}_k^{\,\alpha}(i)\cdot\vec{\phi}_k^{\,\alpha}(j)\,\vec{\phi}_{k'}^{\,\beta}(i)\cdot\vec{\phi}_{k'}^{\,\beta}(j)+(\Delta_{ij}^{kk'}/k_BT)\\&\times\sum_{\alpha,\beta}[\vec{\phi}_k^{\,\alpha}(i)\cdot\vec{\phi}_k^{\,\alpha}(j)\,\vec{\phi}_{k'}^{\,\beta}(i)\cdot\vec{\phi}_{k'}^{\,\beta}(j)+\vec{\phi}_k^{\,\alpha}(i)\cdot\vec{\phi}_{k'}^{\,\alpha}(j)\,\vec{\phi}_{k'}^{\,\beta}(i)\cdot\vec{\phi}_k^{\,\beta}(j)]\Bigg]+\cdots\ ,\end{aligned} \tag{2.4}$$

where i,j run over the magnetic cells, while

$$\Delta_{ij}=\tfrac{1}{2}\sum_{p,p'}[\Delta J_{ip,jp'}^2]_{\rm av}\ , \tag{2.5}$$

$$\Delta_{ij}^{kk'}=\tfrac{1}{2}\sum_{pp'}[\Delta J_{ip,jp'}^2]_{\rm av}F_{kp}F_{k'p'}F_{kp'}F_{k'p}\ , \tag{2.6}$$

$[\ ]_{\rm av}$ stands for a configurational average over the random distribution, $\Delta J=J-[J]_{\rm av}$, and the dots in Eq. (2.4) stand for higher order terms.

Eq. (2.4) was the basis for the analysis in II, where we assumed the $\vec{\phi}_k^{\,\alpha}$'s to be the only relevant order parameters. Our aim in the present study is to allow for spin-glass ordering. Generalizing Ref. 9, we thus define spin-glass variables,

$$\begin{aligned}q_{\mu\nu}^{\alpha\beta}(i)&=\frac{1}{l}\sum_{p}\sigma^{\mu\alpha}(p,i)\sigma^{\nu\beta}(p,i)\\&=\frac{1}{l}\sum_{k}\phi_k^{\mu\alpha}(i)\phi_k^{\nu\beta}(i),\quad\alpha\neq\beta\ ,\end{aligned} \tag{2.7}$$

and

$$\tilde{q}_{\mu\nu}^{\,kk'\alpha\beta}(i)=\frac{1}{\sqrt{2}}[\phi_k^{\mu\alpha}(i)\phi_{k'}^{\nu\beta}(i)+\phi_{k'}^{\mu\alpha}(i)\phi_k^{\nu\beta}(i)]\ ,\qquad\alpha\neq\beta\ ,\quad k\neq k'\ , \tag{2.8}$$

where the indices $\mu,\ \nu=1,\ldots,m$ count components of

the spins within each replica. Note that $q_{\mu\nu}^{\alpha\beta}(i)$ is the cell average of the usual Edwards-Anderson spin-glass order parameter.[3,8,9] Eq. (2.4) can now be written

$$\mathcal{H}_{\text{eff}} = -\frac{1}{2}\sum_{i,j}\sum_{k}[J_{ij}^{kk}]_{\text{av}}\sum_{\alpha}\vec{\phi}_k^{\,\alpha}(i)\cdot\vec{\phi}_k^{\,\alpha}(j) - \frac{1}{2}\sum_{i,j}(\Delta_{ij}/k_BT)\sum_{\mu\nu}\sum_{\alpha\neq\beta}q_{\mu\nu}^{\alpha\beta}(i)q_{\mu\nu}^{\alpha\beta}(j) - \frac{1}{2}\sum_{i,j}\sum_{k\neq k'}(\Delta_{ij}^{kk'}/k_BT)\sum_{\mu\nu}\sum_{\alpha\neq\beta}\tilde{q}_{\mu\nu}^{kk'\alpha\beta}(i) \times \tilde{q}_{\mu\nu}^{kk'\alpha\beta}(j) + \cdots , \tag{2.9}$$

where the dots represent higher order terms. Depending on the strength of the new coupling coefficients $[J_{ij}^{kk}]_{\text{av}}$, Δ_{ij}/k_BT and $\Delta_{ij}^{kk'}/k_BT$ we expect ordering of $\vec{\phi}$, $\tilde{q}$ or q.

The next stage is to transform our spin variables into a continuous form, via a Hubbard transformation.[20] Details of this transformation are given in Appendix A. After showing that $\tilde{q}$ never orders before q, one ends up with a Ginzburg-Landau-Wilson Hamiltonian of the form

$$\overline{\mathcal{H}} = -\frac{1}{2}\int_{\vec{q}}\sum_{k,\alpha}(r_k + A_kq^2 + \cdots)\vec{S}_k^{\alpha}(\vec{q})\cdot\vec{S}_k^{\alpha}(-\vec{q}) - \frac{1}{2}\int_{\vec{q}}(r_Q + A_Qq^2 + \cdots) \times \sum_{\substack{\alpha\neq\beta\\ \mu\nu}}Q_{\mu\nu}^{\alpha\beta}(\vec{q})Q_{\mu\nu}^{\alpha\beta}(-\vec{q}) + \overline{\mathcal{H}}' , \tag{2.10}$$

with $\overline{\mathcal{H}}'$ in Eq. (A9) and r_k, r_Q given in Eq. (A7). From these, one obtains the mean-field temperatures for ordering of $\vec{S}_k$ and of Q,

$$k_BT_c^k = \frac{1}{m}\sum_{j}[J_{ij}^{kk}]_{\text{av}} = \frac{1}{m}\sum_{j}\sum_{pp'}[J_{ip;jp'}]_{\text{av}}F_{kp}F_{kp'} , \tag{2.11}$$

$$(k_BT_c^Q)^2 = (lm^2)^{-1}\sum_{j}\Delta_{ij} = (2lm^2)^{-1}\sum_{j}\sum_{pp'}[\Delta J_{ip;jp'}^2]_{\text{av}} . \tag{2.12}$$

Depending on the relative magnitude of T_c^k and T_c^Q we shall have ordering of the various $\vec{S}_k$'s and of Q. Equality of two (or more) of these temperatures defines multicritical points. For example, $T_c^k = T_c^{k'}$ defines P-F-AF (see Figs. 1 and 2) $T_c^k = T_c^Q$ defines P-SG-F (or P-SG-AF) and $T_c^k = T_c^{k'} = T_c^Q$ defines P-SG-F-AF.

T_c^k and T_c^Q can be changed by changing the relative concentration of the materials forming the alloy. For simplicity we shall restrict ourselves in what follows to a section in the global phase diagram described in Figs. 1 and 2, where there are only two types of magnetic ordering and spin-glass order. For definiteness, we assume that $k=1$ corresponds to ferromagnetic (F), $k=2$ to antiferromagnetic (AF) ordering, and that the other types of antiferromagnetic ordering do not become critical for the considered range of concentrations. In Appendix B we discuss the values of T_c^k and T_c^Q in detail, and show that all the multicritical points in Figs. 1 and 2 are indeed possible. In the specific example discussed in Appendix B we consider a two sublattice antiferromagnetic ordering ($l=2$). Chen and Lubensky[9] treated this ordering with nearest-neighbor (NN) interactions only, and therefore concluded that F and AF orderings cannot coexist. We introduce the next-nearest-neighbor (NNN) interactions, and these make F-AF coexistence possible.

III. MEAN-FIELD THEORY

The "$n\to 0$" method for a random ferromagnet is based on the proof that the free energy per degree of freedom obtained from a partition function of a fictitious system consisting of n identical replicas of the original system is equal, in the limit $n\to 0$, to that of the original system.[22] Mean-field theory approximates the statistical sum involved in the calculation of the partition function by one term, for which the order parameter assumes the value that minimizes the free energy. The question that arises when mean-field theory is applied in the $n\to 0$ limit is what is the correct order of the operations of minimization and taking the limit $n\to 0$. For the ferromagnet (or antiferromagnet) this question is irrelevant, because all the "random terms" in the Hamiltonian are multiplied by n and drop out in the limit $n\to 0$.[1,2] For the spin-glass this question is crucial. We know how to calculate the partition function only for the "replicated" system. If we would know how to calculate the exact free energy of this system we would obtain the correct free energy in the limit $n\to 0$. Note that the EA order parameter $q^{\alpha\beta} = S^{\alpha}S^{\beta}(1-\delta_{\alpha\beta})$ can be defined only for $n\geq 2$. Therefore for systems involving SG we know the partition function only for $n\geq 2$.[23] In the mean-field approximation the partition function is approximated by the most probable term in the statistical sum, hence we should introduce the mean-field approximation and minimize the free energy only for $n\geq 2$. The values of the order parameter for which the minima of the free energy are obtained are then analytically continued to $n=0$. There is no reason to require that the free energy will be a minimum with respect to the order parameter for $n=0$, in this procedure, because the order parameter is constrained to the value obtained by analytic continuation of the value that minimizes the free energy for $n\geq 2$. We assume that if we knew

the correct partition function then the value of the order parameter we obtained by the above analytic continuation would minimize the free energy. The above-described procedure is obviously correct for the paramagnetic phase, where the order parameter vanishes. This enables us to determine the boundaries of the paramagnetic phase. The ordered phases will be studied by a Landau expansion[24] in the vicinity of the paramagnetic phase.

The above considerations lead us to the following recipe in mean-field calculations: (i) Minimize the free energy for $n \geq 2$ and obtain the corresponding values of the order parameters $\tilde{Q}(n)$ and $\tilde{S}(n)$ and the free energy per degree of freedom $\tilde{F}_n$. (ii) Obtain the boundaries between the various phases (that depend on n). (iii) Take the limit $n \to 0$ by which we mean, take $\tilde{Q}(0)$, $\tilde{S}(0)$, and $\tilde{F}_0$, as the mean-field value of the order parameters, and of the free energy per degree of freedom. (iv) Obtain the phase boundaries by substituting $n=0$ in the expressions obtained in (ii). Various justifications were given why this particular extremum should be adopted as the one describing the SG phase: (i) the free energy in the $n \to 0$ limit is not an ordinary Landau free energy, but is defined only for physical values of the order parameter.[17] (ii) Some of the $(n-1)$ factors should be continued to $+1$ in the limit $n \to 0$ to obtain a free energy minimum.[9] (c) The minimization should be done for $n > 1$ and the result analytically continued to $n=0$.[8,25]

Previous works[8,9,17] practically followed the technical steps of this recipe and comparison of the results on the SK model with numerical simulations[17(b)] shows agreement in the vicinity of the paramagnetic phase, although they deviate from the numerical simulation results deep in the ordered phases. In what follows we shall confine ourselves to the neighborhood of the paramagnetic phase.

We next address ourselves to the question of the nature of the SG phase. Following Chen and Lubensky[9] and SK,[17] we assume that the value of $Q_{\mu\nu}^{\alpha\beta}$ in the SG phase is symmetric with respect to the interchange of replicas, $Q_{\mu\nu}^{\alpha\beta} \equiv Q_{\mu\nu}(1-\delta_{\alpha\beta})$, in order to preserve the replicated nature of the Hamiltonian. In a recent publication, de Almeida and Thouless[26] have shown that the extremum symmetric with respect to an interchange of replicas is unstable with respect to breaking of this symmetry. Bray and Moore[27] later found a stable solution resulting from breaking this symmetry, but this involved taking a limit which needs further justification. Recently van Hemmen and Palmer[28] have shown exactly, in the SK model, that the free energy is minimized for a value of the EA order parameter symmetric with respect to replicas interchanges. In a recent letter, Sherrington[29] has shown that the instability found by de Almeida and Thouless[26] for $n=0$ does not occur for $n \geq 2$, where the definition of the EA order parameter is reasonable. Due to the above mentioned prescription we minimize the free energy for $n \geq 2$, therefore this instability does not occur in our calculations. We conclude that the instability with respect to breaking the symmetry between replicas is probably unphysical, and assume the replica symmetric value of the order parameter throughout.

To obtain the MFT (or Landau) equations, we ignore all fluctuations in Eq. (2.10). This amounts to keeping only the zero wave vector ($\vec{q}=0$) terms,

$$\vec{S}_1^{\alpha}(\vec{q}) \to \vec{M}\,\delta(\vec{q}), \quad \vec{S}_2^{\alpha}(\vec{q}) \to \vec{N}\,\delta(\vec{q}) \ , \qquad Q_{\mu\nu}^{\alpha\beta} \to Q_{\mu\nu}(1-\delta_{\alpha\beta})\delta(\vec{q}) \ . \tag{3.1}$$

The MFT free energy in the Ising ($m=1$) case thus becomes [see also Eq. (A9)]

$$F/nk_BT = \tfrac{1}{2}r_1M^2 + \tfrac{1}{2}r_2N^2 + v_{11}M^4 + v_{22}N^4 + 2v_{12}M^2N^2 + (n-1) \times (\tfrac{1}{2}r_QQ^2 + \bar{w}\,Q^3 + w_1QM^2 + w_2QN^2) \ , \tag{3.2}$$

where v_{12} replaces $v_{12} + 2\,\bar{v}_{12}$, $Q \equiv Q_{11}$, and $\bar{w} \equiv w(n-2)$. The minimization of F (for $n \geq 2$) is carried out in detail in Appendix C. Taking the limit $n \to 0$ in the solutions (C4) - (C7), and considering only the vicinity of the paramagnetic phase ($M=N=Q=0$, which exists for $r_1, r_2, r_Q > 0$), the nontrivial phases are the spin-glass (SG),

$$M=N=0, \quad Q=-r_Q/3\,\bar{w} \ , \tag{3.3}$$

existing for $r_1, r_2 > 0$, $r_Q < 0$, the ferromagnet (F),

$$N=0, \quad Q \simeq w_1r_1/(4v_{11}r_Q + 2w_1^2) \ , \qquad M^2 \simeq -r_1r_Q/(4v_{11}r_Q + 2w_1^2) \ , \tag{3.4}$$

existing for $r_1 < 0$, $r_2 > 0$, the antiferromagnet (AF), obtained from F by $M \leftrightarrow N$ and $1 \leftrightarrow 2$, and the mixed phase (M),

$$M^2 \simeq -\frac{w_2^2r_1 - w_1w_2r_2 + 2(v_{22}r_1 - v_{12}r_2)r_Q}{4(w_1^2v_{22} + w_2^2v_{11} - 2v_{12}w_1w_2 + 2Ar_Q)} \ ,$$

$$N^2 \simeq -\frac{w_1^2r_2 - w_1w_2r_1 + 2(v_{11}r_2 - v_{12}r_1)r_Q}{4(w_1^2v_{11} + w_2^2v_{11} - 2v_{12}w_1w_2 + 2Ar_Q)} \ , \tag{3.5}$$

$$Q \simeq \frac{(w_1v_{22} - w_2v_{12})r_1 + (w_2v_{11} - w_1v_{12})r_2}{2(w_1^2v_{22} + w_2^2v_{11} - 2v_{12}w_1w_2 + 2Ar_Q)} \ ,$$

existing for $r_1, r_2 < 0$, $A = v_{11}v_{22} - v_{12}^2 > 0$.

A direct examination of the solutions shows that the $F \leftrightarrow$SG and AF $\leftrightarrow$SG transitions as well as the $M \leftrightarrow F$ and $M \leftrightarrow$AF transitions are continuous. The fact that these transitions are continuous can be shown by showing that the solutions for M (or N) in the mixed phase become imaginary exactly when $M=0$ (or $N=0$) become minima of F. Expressions

for the locations of the transition lines can be easily obtained from Eqs. (3.3)–(3.5). The direct transition $F \leftrightarrow$ AF is first order if $A < 0$. The SG $\leftrightarrow M$ transition occurs continuously on a line where $M^2 = 0$ and $N^2 = 0$, while $Q \neq 0$.

Note that our results for the P, SG, and F phases coincide with those already obtained by Chen and Lubensky,[9] who calculated more terms in the expansion (3.4) and verified the continuity of the $F \leftrightarrow$SG transition. Our calculation reproduces all these results, and in addition verifies that NNN interactions also make all the additional phase diagrams of Figs. 1 and 2 possible.

The only additional complication that arises for the $m > 1$ models relatively to the Ising model are the various relative directions of the magnetization, staggered magnetization and the various "directions" of the spin-glass tensor $Q_{\mu\nu}$. When $N = 0$ or $M = 0$, the analysis of the F, AF, and SG phases follows exactly that of Chen and Lubensky,[9] and will not be reproduced here. In the M phase, when both $\vec{M}$ and $\vec{N}$ are nonzero, the following generalization is necessary: let $\vec{e}^1, \ldots, \vec{e}^m$ be a set of orthogonal unit vectors. Choose $\vec{e}^1$ and $\vec{e}^2$ in the plane determined by $\vec{M}$ and $\vec{N}$, so that $\vec{e}^1$ is in the direction of the bisector of the angle between them. We define θ via

$$\cos\theta = \vec{M}\cdot\vec{e}^1/|\vec{M}| = \vec{N}\cdot\vec{e}^1/|\vec{N}| \ , \tag{3.6}$$

and define

$$\begin{aligned} Q_1 &= \sum_{\mu,\nu=1}^{m} Q_{\mu\nu} e^1_\mu e^1_\nu \ , \\ Q_2 &= \sum_{\mu,\nu=1}^{m} Q_{\mu\nu} e^2_\mu e^2_\nu \ , \\ Q_{12} &= \sum_{\mu,\nu=1}^{m} Q_{\mu\nu} e^1_\mu e^2_\nu \ , \\ Q_3 &= \sum_{\mu,\nu=1}^{m} Q_{\mu\nu} e^\perp_\mu e^\perp_\nu \ , \end{aligned} \tag{3.7}$$

where $\vec{e}^\perp$ is a unit vector orthogonal to $\vec{e}^1$ and $\vec{e}^2$. In terms of these variables, the free energy becomes

$$\begin{aligned} F/nk_BT = {} & \tfrac{1}{2}r_1M^2 + \tfrac{1}{2}r_2N^2 + v_{11}M^4 + v_{22}N^4 + 2v_{12}N^2M^2 + 4\bar{v}_{12}M^2N^2\cos^2 2\theta \\ & + (n-1)\{\tfrac{1}{2}r_Q[Q_1^2 + Q_2^2 + 2Q_{12}^2 + (m-2)Q_3^2] + \bar{w}[Q_1^3 + Q_2^3 + (m-2)Q_3^3] \\ & + w_1M^2(Q_1\cos^2\theta + Q_2\sin^2\theta + Q_{12}\sin 2\theta) + w_2N^2(Q_1\cos^2\theta + Q_2\sin^2\theta - Q_{12}\sin 2\theta)\} \end{aligned} \tag{3.8}$$

Note that the decomposition [(3.6) and (3.7)] is defined only if both M and N do not vanish, i.e., in the mixed phase. If only M (or N) is nonzero then θ is undefined, $\vec{e}^1$ should be chosen in the direction of $\vec{M}$ (or $\vec{N}$), $Q_{12} = 0$, and the last two terms in Eq. (3.8) should be replaced by $w_1M^2Q_1$ (or $w_2N^2Q_1$). This reduces to the analysis of Ref. 9, which is very similar to that of the Ising case presented above. Some details of the mean-field analysis of Eq. (3.8) are presented in Appendix C. We show that the only possible values of the angle θ are $\theta = 0$ ($\vec{M} \| \vec{N}$) or $\theta = \pi/4$ ($\vec{M} \perp \vec{N}$). The former value seems unlikely, if the coefficients in Eq. (3.8) are not too far from their simple initial values [Eq. (A10)]. For the latter value we find $Q_1 = Q_2$ and $Q_{12} \neq 0$. A detailed analysis of this case can be made only if higher order terms in Q_{12} are introduced, and we leave these details for future work. In any case, we conclude that if a mixed phase exists it will most probably have $\vec{M} \perp \vec{N}$, in agreement with our earlier analysis and with many experiments.[2]

IV. RECURSION RELATIONS AND FIXED POINTS

We now analyze the Hamiltonian (2.10) using the renormalization-group technique.[30,31] If r_Q is very large, then the $Q^{\alpha\beta}_{\mu\nu}$ variables can be eliminated from the partition function, and $\bar{\mathcal{H}}$ reduces to the Hamiltonian studied in II, exhibiting the phase diagrams of Fig. 1. We therefore concentrate here on the case when $r_Q \simeq 0$ and spin-glass ordering is important. Once $Q^{\alpha\beta}_{\mu\nu}$ is an important order parameter, the cubic terms in $\bar{\mathcal{H}}'$ [Eq. (A9)] imply that the critical dimensionality is $d_c = 6$, and we concentrate on expansions in $\epsilon = 6 - d$. For $d > 4$, the critical properties near the $F \leftrightarrow P$ and AF $\leftrightarrow P$ transitions are described by mean-field theory, and the quartic terms in Eq. (A9) are irrelevant. Renormalizing the $\vec{S}^\alpha_k$'s ($k = 1, 2$) and the $Q^{\alpha\beta}_{\mu\nu}$'s, Eq. (2.10) can be written

$$\begin{aligned} \bar{\mathcal{H}} = {} & -\tfrac{1}{2}\sum_{k=1}^{2}\int_{\vec{q}}\sum_{\alpha=1}^{n}(r_k + q^2)\vec{S}^\alpha_k(\vec{q})\cdot\vec{S}^\alpha_k(-\vec{q}) - \tfrac{1}{2}\int_{\vec{q}}(r_Q + q^2)\sum_{\substack{\alpha\neq\beta \\ \mu\nu}} Q^{\alpha\beta}_{\mu\nu}(\vec{q})Q^{\alpha\beta}_{\mu\nu}(-\vec{q}) \\ & - \int_{\vec{q}_1}\int_{\vec{q}_2}\left[\sum_{k=1}^{2}\sum_{\substack{\alpha\neq\beta \\ \mu\nu}} w_k Q^{\alpha\beta}_{\mu\nu}(\vec{q}_1)S^{\mu\alpha}_k(\vec{q}_2)S^{\nu\beta}_k(-\vec{q}_1-\vec{q}_2) + w\sum_{\substack{\alpha\neq\beta\neq\gamma \\ \mu\nu\eta}} Q^{\alpha\beta}_{\mu\nu}(\vec{q}_1)Q^{\beta\gamma}_{\nu\eta}(\vec{q}_2)Q^{\gamma\alpha}_{\eta\mu}(-\vec{q}_1-\vec{q}_2)\right] . \end{aligned} \tag{4.1}$$

This is exactly the Hamiltonian considered by Chen and Lubensky.[9] We now follow standard renormalization-group routines,[31] eliminate degrees of freedom with $|\vec{q}| > \Lambda/b$, and rescale $\vec{q} \to b\vec{q}$, $\vec{S}_k^{\alpha} \to \zeta_k \vec{S}_k^{\alpha}$, and $Q_{\mu\nu}^{\alpha\beta} \to \zeta_Q Q_{\mu\nu}^{\alpha\beta}$. Depending on the values of r_1, r_2, and r_Q, various rescaling procedures are adopted.[31] For the SG $\leftrightarrow P$ transition, we rescale $\vec{S}_1^{\alpha}$ and $\vec{S}_2^{\alpha}$ so that r_1 and r_2 remain constant, w_1 and w_2 are irrelevant and the recursion relations and the critical exponents of Ref. 8 are recovered. We now concentrate on the two remaining possibilities, appropriate for the multicritical points P-SG-F and P-SG-F-AF (Fig. 2).

A. *P*-SG-*F* (Paramagnet–spin-glass–ferromagnet)

For the P-SG-F (or P-SG-AF) multicritical point [Fig. 2(a)] we rescale $\vec{S}_2^{\alpha}$ so that r_2 remains constant, hence w_2 becomes irrelevant and the usual rescaling of $\vec{S}_1^{\alpha}$ and $Q_{\mu\nu}^{\alpha\beta}$ yields the recursion relations of Ref. 9, keeping terms up to order ϵ,

$$r_1' = b^{2-\eta_1}\{r_1 - 4(n-1)mw_1^2[A_d - K_d \ln b\,(r_1 + r_Q)]\}\ , \tag{4.2}$$

$$r_Q' = b^{2-\eta_Q}\{r_Q - 36(n-2)mw^2(A_d - 2K_d \ln b\, r_Q) - 4w_1^2[A(0) - 2K_d \ln b\, r_1]\}\ , \tag{4.3}$$

$$w' = b^{\epsilon/2-3\eta_Q/2} \times (w + K_d \ln b\,\{36[(n-3)m+1]w^3 + 4w_1^3/3\})\ , \tag{4.4}$$

$$w_1' = b^{\epsilon/2-\eta_Q/2-\eta_1}\{w_1 + 4K_d \ln b\,[w_1^3 + 3(n-2)mww_1^2]\}\ , \tag{4.5}$$

$$\eta_1 = 4(n-1)mK_d w_1^2/3\ , \tag{4.6}$$

$$\eta_Q = [36(n-2)mw^2 + 4w_1^2]K_d/3\ , \tag{4.7}$$

$$K_d^{-1} = 2^{d-1}\pi^{d/2}\Gamma(d/2),\quad A_d = K_d(1 - b^{4-d})/(d-4)\ . \tag{4.8}$$

In general, apart from complex solutions, these recursion relations have three fixed points of interest, i.e., the Gaussian one, $w^* = w_1^* = 0$, the SG fixed point, $w_1^* = 0$, $(w^*)^2 = \epsilon/36K_d[(4-n)m - 2]$, which coincides with that found in Ref. 8 in the limit $n \to 0$, and a new fixed point, with both w^* and w_1^* nonzero. The first two fixed points are unstable, and it is this third fixed point which should be used to describe the multicritical point P-SG-F [Fig. 2(a)].

Chen and Lubensky[9] substitute $n = 0$ everywhere in the recursion relations, and find the results shown under "Direct $n = 0$" in Table I. The stability exponents of the w and w_1 recursion relations at this third fixed point are $-\epsilon$ and $\lambda_2 < 0$. Linearizing the

TABLE I. Fixed-point values and exponents for P-SG-F.

	"Direct $n=0$"[a]			"Modified $n=0$"		
	$m=1$	$m=2$	$m=3$	$m=1$	$m=2$	$m=3$
$\lvert w^*\rvert(K_d/\epsilon)^{1/2}$	$\frac{1}{6}$	0.0839	0.0614	0.1263	0.0716	0.0547
$\lvert w_1^*\rvert(K_d/\epsilon)^{1/2}$	$\frac{1}{2}$	0.3032	0.2373	0.2797	0.1882	0.1505
λ_2/ϵ	$-\frac{5}{3}$	−1.0791	−0.8686	−0.9149	−0.8301	−0.7816
η_1/ϵ	$-\frac{1}{3}$	−0.2451	−0.2253	0.1043	0.0944	0.0906
η_Q/ϵ	$-\frac{1}{3}$	−0.2149	−0.1960	−0.2787	−0.1987	−0.1849
$(\lambda_t-2)/\epsilon$	$-\frac{8}{3}$	−(1.1501	(−0.9407	0.2933	0.2417	0.2185
$(\lambda_x-2)/\epsilon$	$-\frac{5}{3}$	±0.3247i)	±0.2539i)	−2.1039	−1.3297	−1.1432
$(\nu-\frac{1}{2})/\epsilon$	?	?	?	−0.0733	−0.0605	−0.0546
$(\phi-1)/\epsilon$				−1.1986	−0.7857	−0.6808
a_{t_Q}	2	?	?	0.2706	0.1866	0.1369
a_{x_Q}	1			−7.3906	−5.3598	−4.8709
R	2	?	?	−0.0366	−0.0348	−0.0281

[a]From Ref. 9.

recursion relations for r_1 and r_Q, Chen and Lubensky found complex exponents for $m=2,3$, which are quite unsatisfactory in terms of our physical understanding of the scaling properties near P-SG-F. We shall return to a discussion of related difficulties in Sec. V.

In order to try to avoid the difficulties arising in the direct $n=0$ approach, it is instructive to consider the origins of the various n-dependent factors in the recursion relations, noting the fact that there exists some ambiguity in the analytic continuation to $n \to 0$. The basic idea of the replica method was based on the identity[22]

$$[F]_{\rm av}/mN = \lim_{n\to 0} F_n/nmN \ , \tag{4.9}$$

where F_n is the free energy of the nm-component system, represented by $\overline{\mathcal{H}}$, and $[F]_{\rm av}$ is the averaged free energy of the original system. To obtain the latter, one thus must consider the free energy *per degree of freedom* of the replicated system. Counting degrees of freedom caused no problem until the SG order parameter was introduced. Introduction of $Q^{\alpha\beta}_{\mu\nu}$ artificially added $n(n-1)m^2$ degrees of freedom per site, and various factors of $(n-1)$ result from this "overcounting". When only the SG phase was considered, e.g., in Ref. 8, all these factors can be factored out [see, e.g., Eqs. (3.2) and (3.8)]. Indeed, they also factor out from the recursion relations for r_Q, w, and η_Q, and do not affect the SG $\leftrightarrow P$ critical exponents. However, consider the contributions of order w_1^2 in the recursion relation for r_1 and in η_1. These result from the diagram shown in Fig. 3, i.e., from a summation of the type

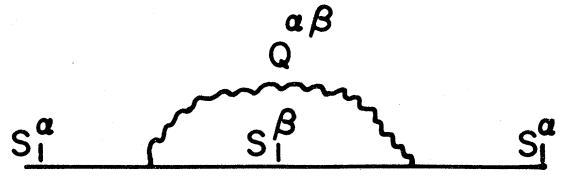

FIG. 3. Diagram contributing the factor $(n-1)$ in Eqs. (4.1) and (4.6) [see Eq. (4.10)]. The wavy line represents a Q propagator, and the straight line represents an S_1 propagator.

$$\int_{\vec q} S_1^\alpha(\vec q) S_1^\alpha(-\vec q) \sum_{\beta\neq\alpha} \int^{>}_{\vec q_1} \langle S_1^\beta(\vec q_1) S_1^\beta(-\vec q_1)\rangle \langle Q^{\alpha\beta}(\vec q_1) Q^{\alpha\beta}(-\vec q_1)\rangle$$
$$= (n-1)\int_{\vec q} S_1^\alpha(\vec q) S_1^\alpha(-\vec q) \int^{>}_{\vec q_1} (r_1+q_1^2)^{-1}(r_Q+q_1^2)^{-1} \ , \tag{4.10}$$

where $\int^{>}_{\vec q}$ means integration over $\Lambda/b < |\vec q| < \Lambda$. Without such terms, the recursion relations for r_1 and η_1 involve only the n ferromagnetic degrees of freedom. The factor $(n-1)$ in Eq. (4.10) simply counts how many spin-glass degrees of freedom one has per ferromagnetic degree of freedom. In the end, we would like to have only one SG degree of freedom per each ferromagnetic one, and this suggests the possibility that these $(n-1)$ factors should be fixed equal to unity. In fact, one can easily check that *all* higher order terms contributing to r_1 and to η_1 will have the same factor of $(n-1)$, for the same reasons.

We therefore conjecture that maybe a "modified $n=0$" procedure has some meaning, i.e., we replace $(n-1)w_1^2$ in Eqs. (4.2) and (4.6) by w_1^2 and only then let $n \to 0$ in the remaining equations. No rigorous justification for this procedure is offered at this stage. With this procedure, the new P-SG-F fixed points values are also given in Table I. Note that all the exponents now become real. We shall show in Sec. V that various additional difficulties are also removed.

B. *P*-SG-*F*-AF
(Paramagnet–spin-glass–ferromagnet–antiferromagnet)

The only addition at the P-SG-F-AF multicritical point is that $\overline{S}_2^\alpha$ also becomes critical, and therefore should also be rescaled by $b^{(d+2-\eta_2)/2}$. The recursion relations for r_1' and w_1', and the expression for η_1, Eqs. (4.2), (4.5), and (4.6), remain unchanged. Similar expressions are now found for r_2', w_2' and η_2, by simply replacing 1 by 2 everywhere. Finally, Eqs. (4.3), (4.4), and (4.7) are modified with w_1^2, $w_1^2 r_1$, and w_1^3 being replaced by $(w_1^2+w_2^2)$, $(w_1^2 r_1 + w_2^2 r_2)$, and $(w_1^3+w_2^3)$, respectively.

The recursion relations for w, w_1, and w_2 have in principle 27 fixed point solutions. Using the modified $n=0$ recursion relations, 15 of these solutions have $w_1^*=0$ or $w_2^*=0$, coinciding with fixed points already discussed above. These solutions are however unstable with respect to w_1 or w_2, respectively. Of the remaining solutions, 10 (or 8, or 4) are complex for the $m=1$ (or $m=2$, or $m=3$) case, and 2 (or 4) are "runaway solutions", i.e., solutions at infinity which can be identified only if higher order terms are included,[1,2] for $m=2$ (or $m=3$). In the case $m=3$ there are also two solutions with $w^*=0$ and $w_1^*=-w_2^*=\pm 0.6124(\epsilon/K_d)^{1/2}$, but these are "unphysical" since they cannot be reached by iterations from our initial Hamiltonian. We are thus left with two solutions for w, $w_1=w_2$, of which we choose the negative ones [see Eq. (A10)]. Values for these solutions are given in Table II. Again, the fixed points are stable, with exponents $-\epsilon$, λ_2, and λ_3.

The situation changes if the direct $n=0$ recursion

TABLE II. Fixed points and exponents for *P*-SG-*F*-AF.

	"Direct $n=0$"			"Modified $n=0$"		
	$m=1$	$m=2$	$m=3$	$m=1$	$m=2$	$m=3$
$\lvert w^*\rvert(K_d/\epsilon)^{1/2}$	0.1491	0.083 33	0.062 35	0.1277	0.073 29	0.055 87
$\lvert w_1^*\rvert(K_d/\epsilon)^{1/2}$	0.3559	0.2500	0.2049	0.2554	0.1788	0.1452
λ_2/ϵ	−1.6667	−1.3333	−1.1276	−1.1304	−0.9970	−0.9104
λ_3/ϵ	0.0780	−0.1667	−0.2482	−0.4348	−0.5437	−0.5842
$\eta_1/\epsilon=\eta_2/\epsilon$	−0.1689	−0.1667	−0.1679	0.0870	0.0852	0.0844
η_Q/ϵ	−0.1958	−0.1667	−0.1679	−0.2174	−0.1726	−0.1685
$(\lambda_t-2)/\epsilon$	−2.5373	−1.3333	−1.0097	0.2865	0.2509	0.2294
$(\lambda_{x_Q}-2)/\epsilon$	−0.8050	−0.8333	−0.8377	−2.2431	−1.4547	−1.2406
$(\lambda_x-2)/\epsilon$	−0.3379	−0.3333	−0.3358	0.1739	0.1705	0.1688
a_{t_Q}	4.3399	2	1.3380	0.4317	0.3147	0.2395
a_{x_Q}	0.9217	1	0.9965	−9.2650	−6.3560	−5.5675
$(\nu-\frac{1}{2})/\epsilon$				−0.0716	−0.0627	−0.0573
$(\phi_Q-1)/\epsilon$	?	?	?	−1.2648	−0.8528	−0.7350
$(\phi-1)/\epsilon$				−0.0563	−0.0402	−0.0303
R_2	0.2124	0.5	0.7447	−21.46	−20.20	−23.25

relations are used: For $m=2$ and $m=3$, 10 of the remaining solutions are complex, and 2 solutions give w and $w_1=w_2$, values of which are listed in Table II. In the case $m=1$, there are six real solutions. Two of these are of the same form as mentioned above, with $w_1=w_2$, and they are also listed in Table II. However, as seen from the table, these solutions seem to be unstable for small ϵ. The remaining four real solutions are nonsymmetric, and have $|w^*|(K_d/\epsilon)^{1/2}=0.1577$, $|w_1^*|(K_d/\epsilon)^{1/2}=0.2536$, and $|w_2^*|(K_d/\epsilon)^{1/2}=0.4562$ (or a permutation of w_1 and w_2). These fixed points are stable, with exponents $-\epsilon$, -1.7292ϵ, and -0.1464ϵ. However, since we find the asymmetry of w_1 and w_2 difficult to accept on physical grounds, we also tabulated the values for the symmetric point. The small values of λ_3 for both fixed points may indicate that higher order terms will restore the stability of the symmetric fixed point at finite values of ϵ.

V. CRITICAL EXPONENTS AND SHAPES OF PHASE DIAGRAMS NEAR THE MULTICRITICAL POINTS

The main difficulty in the determination of the critical exponents of a multicritical point (after finding the appropriate fixed point) has to do with the *identification of the scaling fields.* Temperature and other directly measurable parameters (as concentrations in our case) are usually not the scaling fields, but rather linear combinations (in the asymptotic region) of them. In some simple physical situations, where both competing order parameters are of the same type, physical intuition directs one how to identify the scaling fields.[32,33] In our case, the order parameters are of different types: the F and AF order parameters are vectors, and the SG order parameter is a tensor. Linearization of the recursion relations about the fixed points allows us to identify the asymptotic scaling fields as the eigenvectors of the corresponding eigenvalue exponents. The linearized recursion relations for r_1 and r_Q (or r_1, r_2 and r_Q) near the *P*-SG-*F* (*P*-SG-*F*-AF) fixed point have two (three) eigenvalues and eigenvectors. One of these eigenvalues should be equal to $1/\nu$, and the corresponding eigenvector should describe the *thermal instability,* leading into the paramagnetic phase. We thus identify $\lambda_t=1/\nu$ by identifying the eigenvector which points into the P phase. The remaining eigenvalue(s), equal to $\lambda_x=\phi/\nu$ (and $\lambda_{x_Q}=\phi_Q/\nu$) describes *crossover effects* into a phase where only some of the order parameters (e.g., only $\vec{S}_1^{\alpha}$, $\vec{S}_2^{\alpha}$ or $Q_{\mu\nu}^{\alpha\beta}$) order. The crossover exponents ϕ and ϕ_Q

determine the shape of the phase diagrams near the multicritical points P-SG-F and P-SG-F-AF. In this section we identify these exponents near the P-SG-F and P-SG-F-AF fixed points.

A. P-SG-F

Let the eigenvectors corresponding to λ_t and λ_x be (a_{t_1}, a_{t_Q}) and (a_{x_1}, a_{x_Q}), so that the scaling fields are

$$\begin{aligned} \mu_t &= a_{t_1}\Delta r_1 + a_{t_Q}\Delta r_Q \ , \\ \mu_x &= a_{x_1}\Delta r_1 + a_{x_Q}\Delta r_Q \ . \end{aligned} \tag{5.1}$$

Since we have a freedom of normalization, we can choose $a_{t_1} = a_{x_1} = 1$. Values for a_{t_Q} and a_{x_Q} are given in Table I. For the modified $n = 0$ case, we always have $a_{t_Q} > 0$ and $a_{x_Q} < 0$. This led us to identify λ_t, since we want μ_t to increase when both Δr_1 and Δr_Q increase. The fact that μ_x has opposite signs if Δr_1 or Δr_Q are increased implies that the $F \leftrightarrow P$ and the SG $\leftrightarrow P$ phase boundaries should be on opposite sides of the μ_t axis, yielding a phase diagram like that shown in Fig. 4(a). The resulting exponents ν and ϕ are also given in Table I. Since the shape of the transition lines near P-SG-F is given by

$$\mu_x = A_1 \mu_t^{\phi}, \quad \mu_x = A_Q \mu_t^{\phi} \ , \tag{5.2}$$

and since for small ϵ we find $\phi < 1$, we conclude that the lines approach the P-SG-F point tangentially to the μ_x direction. The amplitudes A_1 and A_Q are nonuniversal, but their ratio is universal, given by

$$R = \frac{A_Q}{A_1} = \frac{a_{t_Q}}{a_{x_Q}} + O(\epsilon) \ . \tag{5.3}$$

Zero order values of R are also given in Table I. Note that $R < 0$, as it should be in order that μ_t indeed goes into the P phase.

Thus far we described only the results from the modified $n = 0$ calculation. If we use the direct $n = 0$ approach, the calculation probably becomes meaningless for $m = 2, 3$ due to the complex exponents.

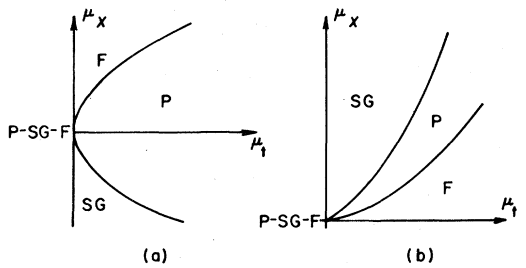

FIG. 4. The shape of the critical lines in the vicinity of the P-SG-F multicritical point. (a) Using the "modified $n = 0$" calculation. (b) Using the "direct $n = 0$" analysis.

However, it should be emphasized that even the case $m = 1$ does not lead to satisfactory results: the ratio R turns out to be positive, implying a phase diagram of the shape shown in Fig. 4(b). There is no way to identify an eigenvector pointing into the paramagnetic phase, and both transition lines appear between the two scaling field directions. For this reason, we have doubts about Chen and Lubensky's[9] identification of the exponents ν and ϕ in this case.

B. P-SG-F-AF

We now have three scaling fields, μ_t, μ_{x_1}, and μ_{x_2}. It turns out that in almost all cases, two eigenvectors are symmetric with respect to exchange of Δr_1 and Δr_2, while the last one is always antisymmetric with respect to this exchange. Thus, the scaling fields are found to have the general form

$$\begin{aligned} \mu_t &= \Delta r_1 + \Delta r_2 + a_{t_Q}\Delta r_Q \ , \\ \mu_{x_Q} &= \Delta r_1 + \Delta r_2 + a_{x_Q}\Delta r_Q \ , \\ \mu_x &= \Delta r_1 - \Delta r_2 \ . \end{aligned} \tag{5.4}$$

The corresponding eigenvalues and values of a_{t_Q} and a_{x_Q} are given in Table II. Again, in the modified $n = 0$ analysis we identify the thermal eigenvalue $\lambda_t = 1/\nu$ through $a_{t_Q} > 0$. The crossover to the surface of $P \to$ SG ordering or to the line P-F-AF of $P \to M$ ordering (with $r_1 \equiv r_2$) is described by $\lambda_{x_Q} = \phi_Q/\nu$, and the crossover to the surfaces of $P \to F$ or $P \to$ AF ordering is described by $\lambda_x = \phi/\nu$.

Viewed from the direction of the paramagnetic phase, the P-SG-F-AF point is surrounded by surfaces of $P \to F$, $P \to$ AF, $P \to$ SG transitions [see Fig. 2(b)]. These surfaces intersect on lines of P-SG-F, P-SG-AF, or P-F-AF points. In order to find these surfaces, we first solve Eq. (5.4) for Δr_1, Δr_2, and Δr_Q, in terms of μ_t, μ_{x_Q}, and μ_x. Under RG iterations, μ_t, μ_{x_Q}, and μ_x transform into $\mu_t b^{1/\nu}$, $\mu_{x_Q} b^{\lambda_{x_Q}}$, and $\mu_x b^{\lambda_x}$. Fixing b by demanding that the Δr corresponding to a noncritical variable be of order unity, and equating the one corresponding to a critical order parameter to zero, yields expressions for the various surfaces:

$$\begin{aligned} &P \to \text{SG}, \quad \mu_{x_Q} = A\,\mu_t^{\phi_Q} \ , \\ &P \to F(\text{AF}), \quad \mu_x = \pm(B\mu_t^{\phi} + C\mu_{x_Q}\mu_t^{\phi - \phi_Q}) \ , \end{aligned} \tag{5.5}$$

with the universal ratios

$$\begin{aligned} R_1 &= -(B + C)/A = -1 + O(\epsilon) \ , \\ R_2 &= -B/C = a_{x_Q}/a_{t_Q} + O(\epsilon) \ . \end{aligned} \tag{5.6}$$

Zero order values of R_2 are also given in Table II.

The results presented in Table II for the modified $n = 0$ calculation cause no problem: the thermal

eigenvalue is easily identified, and all the critical surfaces approach the P-SG-F-AF point from reasonable directions. This is not the case for the direct $n=0$ calculation, where again we find that both a_{t_Q} and a_{x_Q} are positive and phase diagrams like that shown in Fig. 4(b) are implied. Moreover, the case $m=1$ is even more tricky: the symmetric fixed point, given in Table II, leads to the same difficulties as for $m=2,3$. For the nonsymmetric one, it is again difficult to give the results a satisfactory physical interpretation: the eigenvalues are $(\lambda_i-2)/\epsilon=-1.2592$, -2.6250, -0.1905, and the corresponding eigenvectors are (1, 0.2001, 0.8461), (1, 0.2607, 2.4870), (1, -5.9240, -0.4378).

VI. DISCUSSION

In this work we studied the critical properties of random alloys which may exhibit SG ordering. By MFT we calculated (Sec. III) the global phase diagram of such a random alloy, i.e., the transition temperatures between the various phases as a function of the averaged exchange couplings and of the variances of these couplings. It was shown that *all the phase diagrams of Figs. 1 and 2 can in principle be realized* as particular cuts of the global phase diagram. NNN exchange interactions were shown to be crucial for the realization of some phase diagrams. We have demonstrated explicitly (Appendix B) that a mixture of a ferromagnet with a two sublattice antiferromagnet will exhibit a SG phase, if the NNN interactions are weak compared to the variance of the interactions strength. Otherwise coexistence of ferromagnetic and antiferromagnetic ordering is possible. This can be understood by the following intuitive argument: the NN interactions are the interactions between the sublattices, while the NNN interactions are the interactions between spins in the same sublattice, possibly favoring *both* F and AF ordering. At the P-F-AF multicritical point, the average NN interaction vanishes and the F and AF orderings are degenerate, but $T_c^F=T_c^{\mathrm{AF}}>0$ due to the NNN interactions. If the variance of the interactions is large compared to NNN interactions, it will tend to break the sublattices locally and lead to SG ordering [Fig. 2(a)]. If the variance of the interactions is small — the P-F-AF multicritical point will be obtained [Figs. 1(a) and 1(b)]. In many previous theoretical studies the NNN interactions were ignored leading to the phase diagram of Fig. 1(c) or to that of Fig. 2(a). All experiments of which we are aware (which were discussed in II), except one,[34] lead to phase diagrams of the type shown in Fig. 1(a). We conclude that the NNN interactions are essential for the study of phase diagrams of F-AF random alloys. In order to obtain experimentally a SG phase in F-AF alloy we should mix materials with weak NNN interactions, or with AF NNN interactions.[35] In order to approach experimentally the P-SG-F-AF multicritical point, one should mix alloys exhibiting the phase diagram of Fig. 1(a) with alloys exhibiting the phase diagram of Fig. 2(a), i.e., one has to mix at least three components [Fig. 2(b)]. We assumed that the lattice structure of all the components mixed to form the alloy is the same, therefore materials mixed to form these alloys should have this property, in order to avoid structural effects.

A few words should be said here concerning the assumptions of the present calculations. The main assumptions have to do with the replica technique and with the SG order parameters. Sec. III contains a detailed discussion of our MFT calculation in the limit $n\to 0$, and we need not repeat it here. In view of existing experience, we are inclined to believe that the qualitative features of the phase diagrams come out correctly. In Secs. IV and V we showed that the direct substitution of $n=0$ in the recursion relations yields "unphysical" phase diagrams. A modified calculation was suggested, which gave much more aesthetic results. We offer no real justification for this procedure except for the heuristic arguments presented in Sec. IV. Moreover, recent diagrammatic expansions which avoid the replica method[36] seem to reproduce the direct $n=0$ results of Ref. 9. If the direct $n=0$ results should indeed be used, then our calculations leave many open questions, mainly concerning the detailed structure of the phase diagrams near the multicritical points. Probably, there is no escape from having regions in which ordered phases appear at temperatures higher than those in which the disordered paramagnetic phase appears.

Another question concerns the relevance of results obtained in $6-\epsilon$ dimensions to three dimensions. It has recently been shown,[37] that the quartic terms in $Q_{\mu\nu}^{\alpha\beta}$, which are irrelevant near the $P\to$SG fixed point in $6-\epsilon$ dimensions, remain irrelevant even below four dimensions for $m>m^*$, with $2<m^*<3$ to order $\epsilon=6-d$. If these results are also relevant for the P-SG-F and P-SG-F-AF fixed points, then the qualitative features found near these fixed points may be relevant for real systems. Moreover, since at $d=3$ one has $\epsilon=6-d=3$, it is impossible to know if the difficulties found near $d=6$ using the direct $n=0$ calculation will persist down to $d=3$.

In any case, although the present study leaves many quantitative questions for real systems unanswered, its importance is in pointing at the qualitative possibilities. Experiments and direct three dimensional calculations should check how many of these are really realized.

ACKNOWLEDGMENT

This research was supported in part by a grant from the United States - Israel Binational Science Foundation (BSF), Jerusalem, Israel.

APPENDIX A: CONTINUOUS-SPIN HAMILTONIAN

We wish to replace the trace over the fixed length variables $\vec{\sigma}(p,i)$ by an integral over continuous variables. Using the standard identity

$$\exp\left[\frac{1}{2}\sum_{i,j} S_i A_{ij} S_j\right] \equiv C\int \left(\prod_i dx_i\right) \exp\left[-\frac{1}{2}\sum_{i,j} x_i (A^{-1})_{ij} x_j + \sum_i x_i S_i\right] \tag{A1}$$

for each of the terms in Eq. (2.9), we find

$$Z = \int \left[\prod_{i,\alpha,\mu} dS_\mu^\alpha(i)\right]\left[\prod_{\substack{i,\alpha\neq\beta\\ \mu\nu}} dQ_{\mu\nu}^{\alpha\beta}(i)\right]\left[\prod_{\substack{i,\alpha\neq\beta\\ \mu,\nu,k,k'}} d\tilde{Q}_{\mu\nu}^{kk'\alpha\beta}(i)\right] \exp(\bar{\mathcal{H}}) \ , \tag{A2}$$

with

$$\bar{\mathcal{H}} = -\frac{1}{2}\sum_{i,j}\sum_k K_{ij}^k \sum_\alpha \vec{S}_k^\alpha(i)\cdot\vec{S}_k^\alpha(j) - \frac{1}{2}\sum_{i,j} L_{ij} \sum_{\substack{\alpha\neq\beta\\ \mu,\nu}} Q_{\mu\nu}^{\alpha\beta}(i) Q_{\mu\nu}^{\alpha\beta}(j) - \frac{1}{2}\sum_{i,j}\sum_{k,k'} L_{ij}^{kk'} \sum_{\substack{\alpha\neq\beta\\ \mu,\nu}} \tilde{Q}_{\mu\nu}^{kk'\alpha\beta}(i)\,\tilde{Q}_{\mu\nu}^{kk'\alpha\beta}(j)$$

$$+\ln \mathrm{Tr}_{\{\vec{\sigma}\}} \exp\left[\sum_i\left[\sum_{\alpha,k}\vec{S}_k^\alpha(i)\cdot\vec{\phi}_k^\alpha(i) + \sum_{\substack{\alpha\neq\beta\\ \mu\nu}} Q_{\mu\nu}^{\alpha\beta}(i) q_{\mu\nu}^{\alpha\beta}(i) + \sum_{\alpha\neq\beta}\sum_{kk'} \tilde{Q}_{\mu\nu}^{kk'\alpha\beta}(i)\,\tilde{q}_{\mu\nu}^{kk'\alpha\beta}(i)\right]\right] \ , \tag{A3}$$

where

$$K_{ij}^k \equiv \{([J_{ij}^{kk}]_{\mathrm{av}})^{-1} k_B T\}_{ij} \ ,$$

$$L_{ij} \equiv [(\Delta_{ij})^{-1}(k_B T)^2]_{ij} \ ,$$

etc., and $\bar{\mathcal{H}}$ is given up to an additive constant. To perform the trace over $\vec{\sigma}$ we now expand the exponential in Eq. (A3). Using the identities[38]

$$\begin{aligned}
&\mathrm{Tr}_{\vec{\sigma}}[\phi_k^{\mu\alpha}(i)\phi_{k'}^{\mu\alpha}(i)] = \delta_{kk'}/m \ ,\\
&\mathrm{Tr}_{\vec{\sigma}}[q_{\mu\nu}^{\alpha\beta}(i) q_{\mu\nu}^{\alpha\beta}(i)] = 1/lm^2 \ ,\\
&\mathrm{Tr}_{\vec{\sigma}}(\tilde{q}_{\mu\nu}^{kk'\alpha\beta}\,\tilde{q}_{\mu\nu}^{kk'\alpha\beta}) = 1/m^2 \ ,\\
&\mathrm{Tr}_{\vec{\sigma}}(q_{\mu\nu}^{\alpha\beta} q_{\nu\eta}^{\beta\gamma} q_{\eta\mu}^{\gamma\alpha}) = 1/l^2 m^3 \ ,\\
&\mathrm{Tr}_{\vec{\sigma}}(q_{\mu\nu}^{\alpha\beta}\phi_k^{\mu\alpha}\phi_k^{\nu\beta}) = 1/lm^2 \ ,\\
&\mathrm{Tr}_{\vec{\sigma}}(\phi_{(i)}^{\mu\alpha}\phi_{(i)}^{\mu\alpha}\phi_{(i)}^{\nu\alpha}\phi_{(i)}^{\nu\alpha}) = (1+2\delta_{\mu\nu})/lm(m+2) + (l-1)/lm^2 \ ,
\end{aligned} \tag{A4}$$

etc., we end up with

$$\bar{\mathcal{H}} = -\frac{1}{2}\sum_{i,j}\sum_k K_{ij}^k \sum_\alpha \vec{S}_k^\alpha(i)\cdot\vec{S}_k^\alpha(j) - \frac{1}{2}\sum_{i,j} L_{ij} \sum_{\substack{\alpha\neq\beta\\ \mu,\nu}} Q_{\mu\nu}^{\alpha\beta}(i) Q_{\mu\nu}^{\alpha\beta}(j) - \frac{1}{2}\sum_{i,j}\sum_{k,k'} L_{ij}^{kk'} \sum_{\substack{\alpha\neq\beta\\ \mu,\nu}} \tilde{Q}_{\mu\nu}^{kk'\alpha\beta}(i)\,\tilde{Q}_{\mu\nu}^{kk'\alpha\beta}(j)$$

$$+\frac{1}{2m}\sum_i\sum_{\alpha\kappa}|\vec{S}_k^\alpha(i)|^2 + \frac{1}{2lm^2}\sum_i\sum_{\substack{\alpha\neq\beta\\ \mu\nu}}[Q_{\mu\nu}^{\alpha\beta}(i)]^2 + \frac{1}{2m^2}\sum_i\sum_{\substack{\alpha\neq\beta\\ \mu\nu}}\sum_{k\neq k'}[\tilde{Q}_{\mu\nu}^{kk'\alpha\beta}(i)]^2 + \cdots \ . \tag{A5}$$

Fourier transforming the variables, $\vec{S}_k^\alpha(i) \to \vec{S}_k^\alpha(\vec{q})$, etc., we find

$$\bar{\mathcal{H}} = -\frac{1}{2}\int_{\vec{q}}\sum_{k,\alpha}(r_k + A_k q^2 + \cdots)\vec{S}_k^\alpha(\vec{q})\cdot\vec{S}_k^\alpha(-\vec{q}) - \frac{1}{2}\int_{\vec{q}}(r_Q + A_Q q^2 + \cdots)\sum_{\substack{\alpha\neq\beta\\ \mu\nu}} Q_{\mu\nu}^{\alpha\beta}(\vec{q}) Q_{\mu\nu}^{\alpha\beta}(-\vec{q})$$

$$-\frac{1}{2}\int_{\vec{q}}\sum_{k\neq k'}(\tilde{r}_Q^{\,kk'} + \tilde{A}_Q^{\,kk'} q^2 + \cdots)\sum_{\substack{\alpha\neq\beta\\ \mu,\nu}} \tilde{Q}_{\mu\nu}^{kk'\alpha\beta}(\vec{q})\,\tilde{Q}_{\mu\nu}^{kk'\alpha\beta}(-\vec{q}) + \bar{\mathcal{H}}' \ , \tag{A6}$$

where $\int_{\vec{q}} \equiv (a/2\pi)^d \int d^d q$ with $|\vec{q}| < \Lambda$, $\bar{\mathcal{H}}'$ includes the higher order terms, and

$$r_k = [k_B T/\hat{J}_k(0) - 1/m](a/2\pi)^d \ ,$$
$$r_Q = [(k_B T)^2/\hat{\Delta}(0) - 1/lm^2](a/2\pi)^d \ , \tag{A7}$$
$$\tilde{r}_Q^{kk'} = [(k_B T)^2/\hat{\Delta}^{kk'}(0) - 1/m^2](a/2\pi)^d \ ,$$

etc. (a is the size of the magnetic unit cell), while $\hat{J}_k(\vec{q})$, $\hat{\Delta}(\vec{q})$, and $\hat{\Delta}^{kk'}(\vec{q})$ are the Fourier transforms of $[J_{ij}^{kk}]_{\rm av}$, Δ_{ij}, and $\Delta_{ij}^{kk'}$. From the definitions (2.5) and (2.6) it is obvious that

$$\Delta_{ij} > l^2 \Delta_{ij}^{kk'} \ . \tag{A8}$$

Therefore, one always has $r_Q < \tilde{r}_Q^{kk'}$, and Q always orders before $\tilde{Q}$. We can therefore treat $\tilde{Q}$ with a perturbation expansion, and eliminate it from $\bar{\mathcal{H}}$. This will result in some shifts in the coefficients of $\bar{\mathcal{H}}'$. Explicitly, $\bar{\mathcal{H}}'$ has the form

$$\begin{aligned}\bar{\mathcal{H}}' = -\sum_\alpha \int_{\vec{q}_1}\int_{\vec{q}_2}\int_{\vec{q}_3} \Bigg(&\sum_k v_{kk}\vec{S}_k^\alpha(\vec{q}_1)\cdot\vec{S}_k^\alpha(\vec{q}_2)\vec{S}_k^\alpha(\vec{q}_3)\cdot\vec{S}_k^\alpha(-\vec{q}_1-\vec{q}_2-\vec{q}_3) \\ &+2\sum_{k\neq k'} v_{kk'}\vec{S}_k^\alpha(\vec{q}_1)\cdot\vec{S}_k^\alpha(\vec{q}_2)\vec{S}_{k'}^\alpha(\vec{q}_3)\cdot\vec{S}_{k'}^\alpha(-\vec{q}_1-\vec{q}_2-\vec{q}_3) \\ &+4\sum_{k\neq k'} \bar{v}_{kk'}\vec{S}_k^\alpha(\vec{q}_1)\cdot\vec{S}_{k'}^\alpha(\vec{q}_2)\vec{S}_k^\alpha(\vec{q}_3)\cdot\vec{S}_{k'}^\alpha(-\vec{q}_1-\vec{q}_2-\vec{q}_3)\Bigg) \\ -w\sum_{\mu\nu\eta}\sum_{\alpha\beta\gamma}\int_{\vec{q}_1}\int_{\vec{q}_2} &Q_{\mu\nu}^{\alpha\beta}(\vec{q}_1)Q_{\nu\eta}^{\beta\gamma}(\vec{q}_2)Q_{\eta\mu}^{\gamma\alpha}(-\vec{q}_1-\vec{q}_2) \\ -\sum_k w_k\sum_{\mu\nu}\sum_{\alpha\beta}\int_{\vec{q}_1}\int_{\vec{q}_2} &Q_{\mu\nu}^{\alpha\beta}(\vec{q}_1)S_k^{\mu\alpha}(\vec{q}_2)S_k^{\nu\beta}(-\vec{q}_1-\vec{q}_2)+\cdots \ ,\end{aligned} \tag{A9}$$

with (if we ignore the shift resulting from the elimination of $\tilde{Q}$ and of irrelevant AF orderings)

$$v_{kk} = v_{kk'} = \bar{v}_{kk'} = [4lm^2(m+2)]^{-1}(a/2\pi)^{3d} \ ,$$
$$w = -l^{-2}m^{-3}(a/2\pi)^{2d}, \quad w_k = -(6lm^2)^{-1}(a/2\pi)^{2d} \ , \tag{A10}$$

etc. One can easily check that the elimination of $\tilde{Q}$ leads to a negative shift in $v_{kk'}$ leaving unaffected v_{kk} and $\bar{v}_{kk'}$. Note that the signs of w and w_k are arbitrary, since we could write Eq. (A3) with the opposite signs in the exponential. We choose the signs to be as indicated in Eq. (A10), in order to have positive values of $\langle Q^{\alpha\beta}\rangle$ generated by ordering of $\langle S^\alpha\rangle$.

The explicit form for $\bar{\mathcal{H}}$ given here contains only second cumulants of the distribution of the random exchange variables. If this distribution is non-Gaussian then higher cumulants will contribute to the various coefficients. These are irrelevant, unless they cause a vanishing of some of the coefficients already given, in which case higher-order critical points may arise.[8] We ignore these possibilities here.

APPENDIX B: INFLUENCE OF NNN INTERACTIONS

In this Appendix, we work out a simple example, demonstrating that all the sections of the phase diagram depicted in Figs. 1 and 2 can in principle be obtained in experiments. Assume we treat a d-dimensional lattice with NN and NNN interactions only. We investigate concentrations for which only the ferromagnetic ($k=1$) and the simple two sublattice antiferromagnetic ($k=2$) types of order are relevant, so that $l=2$. In this case [See Eqs. (2.11) and (2.12)],

$$k_B T_C^1 = (C_1[J_1]_{\rm av} + C_2[J_2]_{\rm av})/m \ ,$$
$$k_B T_C^2 = (-C_1[J_1]_{\rm av} + C_2[J_2]_{\rm av})/m \ , \tag{B1}$$
$$k_B T_C^Q = \{(C_1[\Delta J_1^2]_{\rm av} + C_2[\Delta J_2^2]_{\rm av})/2m^2\}^{1/2} \ ,$$

where J_1 and J_2 are the NN and NNN exchange coefficients and C_1 and C_2 are the corresponding coordination numbers [for a hypercubic lattice, $C_1 = 2d$ and $C_2 = 2d(d-1)$].

If $J_2 = 0$ then clearly T_C^1 can be equal to T_C^2 only if $T_C^1 = T_C^2 = 0$, whereas $T_C^Q > 0$. Therefore, Fig. 2(a) results, as found by Chen and Lubensky.[9] If NNN interactions are introduced then $T_C^1 = T_C^2$ implies $[J_1]_{\rm av} = 0$, $k_B T_C^1 = k_B T_C^2 = C_2[J_2]_{\rm av}/m$. This may be higher than $k_B T_C^Q$, implying the phase diagram of Fig. 1(a).

Assuming a probability p_1 that $J_1 = J_F > 0$ and a probability $1-p_1$ that $J_1 = J_A < 0$, we find

$$[J_1]_{\rm av} = p_1 J_F + (1-p_1)J_A \ , \tag{B2}$$

so that $T_C^1 = T_C^2$ for $p_1 = J_A/(J_A - J_F)$. If $J_2 > 0$ is not

sensitive to the identity of the ions then $k_B T_C^1 = k_B T_C^2 \simeq C_2 J_2/m$, $k_B T_C^Q \simeq (C_1 J_F |J_A|/2m^2)^{1/2}$, and one can estimate when $T_C^1 = T_C^2 > T_C^Q$. Thus, a ferromagnetic average NNN interaction favors a situation where the F and AF phases coexist. If we introduce an additional component into the alloy, reducing the average NNN interaction, one may reach — as a function of the concentration p of this ingredient — a point at which $T_C^1 = T_C^2 = T_C^Q$,[2] i.e., the point P-SG-F-AF [Fig. 2(b)]. The global phase diagram, exhibiting all possible multicritical points, can thus be realized in the $T - p_1 - p_2$ space.

APPENDIX C: MINIMA OF THE FREE ENERGY

In this Appendix we follow the recipe outlined in Sec. III, minimize the free energies (3.2) and (3.8) for $n > 2$ and let $n \to 0$.

For the Ising ($m = 1$), Eq. (3.2) yields

$$\frac{\partial(F/nk_BT)}{\partial M} = [r_1 + 4v_{11}M^2 + 4v_{12}N^2 + 2(n-1)w_1 Q]M = 0 \ , \tag{C1}$$

$$\frac{\partial(F/nk_BT)}{\partial N} = [r_2 + 4v_{22}N^2 + 4v_{12}M^2 + 2(n-1)w_2 Q]N = 0 \ , \tag{C2}$$

$$\frac{\partial(F/nk_BT)}{\partial Q} = (n-1)(r_Q Q + 3\bar{w}\, Q^2 + w_1 M^2 + w_2 N^2) = 0 \ . \tag{C3}$$

The extrema are thus as follows: paramagnet (P),

$$M = N = Q = 0 \ , \tag{C4}$$

spin glass (SG),

$$M = N = 0, \quad Q = -r_Q/3\bar{w} \ , \tag{C5}$$

ferromagnet (F),

$$\begin{aligned} &N = 0, \quad Q = (-b_1 \pm \Delta_1)/6\bar{w} \ , \\ &M^2 = -[r_1 + 2(n-1)w_1 Q]/4v_{11} \ , \\ &b_1 = r_Q - (n-1)w_1^2/(2v_{11}) \ , \\ &\Delta_1 = (b_1^2 + 3\bar{w}\, w_1 r_1/v_{11})^{1/2} \ , \end{aligned} \tag{C6}$$

antiferromagnet (AF), replace $N \leftrightarrow M$, $2 \leftrightarrow 1$ in Eq. (C6), and mixed (M),

$$\begin{aligned} &Q = [-b \pm (b^2 + 12\bar{w}\, C)^{1/2}]/6\bar{w} \ , \\ &b = r_Q - (n-1)(w_1^2 v_{22} + w_2^2 v_{11} - 2v_{12}w_1 w_2)/2A \ , \\ &C = [(w_1 v_{22} - w_2 v_{12})r_1 + (w_2 v_{11} - w_1 v_{12})r_2]/4A \ , \\ &M^2 = [r_2 v_{12} - r_1 v_{22} + 2(n-1)(v_{12}w_2 - v_{22}w_1)Q]/2A \ , \\ &N^2 = [r_1 v_{12} - r_2 v_{11} + 2(n-1)(v_{12}w_1 - v_{11}w_2)Q]/2A \ , \\ &A = v_{11}v_{22} - v_{12}^2 \ . \end{aligned} \tag{C7}$$

These solutions are minima if the determinants of all the principal minors of the matrix of the second derivatives of F with respect to M, N and Q are positive definite. Clearly, P is a minimum if $r_1, r_2, r_Q > 0$, and SG is a minimum if $r_1, r_2 > 0$ and $r_Q < 0$. To discuss F, replace Eq. (C1) by (note that $N = 0$ and $r_2 > 0$ in F)

$$\frac{\partial(F/nk_BT)}{\partial M^2} = \tfrac{1}{2}r_1 + 2v_{11}M^2 + (n-1)w_1 Q \ . \tag{C8}$$

The appropriate second derivatives are

$$\begin{aligned} &\frac{\partial^2(F/nk_BT)}{\partial(M^2)^2} = 2v_{11}, \quad \frac{\partial^2(F/nk_BT)}{\partial M^2 \partial Q} = (n-1)w_1 \ , \\ &\frac{\partial^2(F/nk_BT)}{\partial Q^2} = (n-1)(r_Q + 6\bar{w}\, Q) \\ &\qquad = (n-1)[(n-1)w_1^2/2v_{11} \pm \Delta_1] \ , \end{aligned} \tag{C9}$$

and the appropriate determinants are

$$d_1 = 2v_{11}, \quad d_2 = \pm 2v_{11}(n-1)\Delta_1 \ . \tag{C10}$$

Hence, for $n \geq 2$, we must choose the positive sign of Δ_1 in Eq. (C6).

The calculation for AF is similar. For M, we can consider derivatives with respect to both M^2 and N^2. The resulting determinants are

$$d_1 = 2v_{11}, \quad d_2 = 4A, \quad d_3 = \pm 4A(n-1)\Delta \ , \tag{C11}$$

where $\Delta = (b^2 + 12\bar{w}\, C)^{1/2}$ is the square root appearing in Eq. (C7). Again, we conclude that the positive sign of this square root must be chosen. In addition, we conclude that the mixed phase exists only if $A > 0$. This condition is the same as noted in II for obtaining the phase diagram of Fig. 1(a). If $A < 0$ then Fig. 1(b) results.

In the vicinity of the paramagnetic phase, r_1, r_2, or r_Q are small. Expanding Eqs. (C6) and (C7) in powers of these, putting the positive signs for Δ_1 and for Δ and letting $n \to 0$ yields Eqs. (3.4) and (3.5).

Note that the transition $F \to P$ (or AF $\to P$) is second order only for $b_1 > 0$. For $n > 1$, if r_Q is small, b_1 can be negative and therefore Eq. (C6) can not be used to determine Q. Higher-order terms in M and Q must be added to F in order to find details of the transition, which will have to be first order. This need not worry us in the limit $n \to 0$.

We now turn to the case $m > 1$. The equations for the extrema of F [Eq. (3.8)] in the M phase now

become,

$$\frac{\partial(F/nk_BT)}{\partial M^2}=\tfrac{1}{2}[r_1+4v_{11}M^2+4v_{12}N^2+8\bar{v}_{12}N^2\cos^2 2\theta+2(n-1)w_1(Q_1\cos^2\theta+Q_2\sin^2\theta+Q_{12}\sin 2\theta)]=0\ , \quad \text{(C12)}$$

$$\frac{\partial(F/nk_BT)}{\partial N^2}=\tfrac{1}{2}[r_2+4v_{22}N^2+4v_{12}M^2+8\bar{v}_{12}M^2\cos^2 2\theta+2(n-1)w_2(Q_1\cos^2\theta+Q_2\sin^2\theta-Q_{12}\sin 2\theta)]=0\ , \quad \text{(C13)}$$

$$\frac{\partial(F/nk_BT)}{\partial Q_1}=(n-1)[r_QQ_1+3\bar{w}Q_1^2+(w_1M^2+w_2N^2)\cos^2\theta]=0\ , \quad \text{(C14)}$$

$$\frac{\partial(F/nk_BT)}{\partial Q_2}=(n-1)[r_QQ_2+3\bar{w}Q_2^2+(w_1M^2+w_2N^2)\sin^2\theta]=0\ , \quad \text{(C15)}$$

$$\frac{\partial(F/nk_BT)}{\partial Q_{12}}=(n-1)[2r_QQ_{12}+(w_1M^2-w_2N^2)\sin 2\theta]=0\ , \quad \text{(C16)}$$

$$\frac{\partial(F/nk_BT)}{\partial Q_3}=(n-1)[r_QQ_3+3(m-2)\bar{w}Q_3^2]=0\ , \quad \text{(C17)}$$

$$\frac{\partial(F/nk_BT)}{\partial\theta}=-8\bar{v}_{12}M^2N^2\sin 4\theta+(n-1)[(w_1M^2+w_2N^2)(Q_2-Q_1)\sin 2\theta+2(w_1M^2-w_2N^2)Q_{12}\cos 2\theta]=0\ . \quad \text{(C18)}$$

Substitution of Eqs. (C14)–(C16) in Eq. (C18) yields

$$\{[r_Q+3\bar{w}(Q_1+Q_2)][(n-1)(w_1M^2-w_2N^2)^2+16v_{12}M^2N^2r_Q]-(n-1)r_Q(w_1M^2+w_2N^2)^2\}\sin 4\theta=0\ , \quad \text{(C19)}$$

hence $\theta=0$ ($\vec{M}\parallel\vec{N}$) or $\theta=\frac{1}{4}\pi$ ($\vec{M}\perp\vec{N}$). In order to determine which ordering actually occurs one should examine the matrix of the second derivatives, in both cases.

For $\theta=0$,

$$\frac{\partial^2(F/nk_BT)}{\partial\theta^2}=2(n-1)(Q_2-Q_1)(w_1M^2+w_2N^2)-32\bar{v}_{12}M^2N^2\ , \quad \text{(C20)}$$

and all mixed second derivatives with respect to θ and one of the other variables vanish. Thus, if Eq. (C20) gives a negative result, then we need not consider $\theta=0$ any further. If Eq. (C20) gives a positive result, we must consider the remaining variables. If $\theta=0$ then $Q_{12}=0$ and the equations for Q_2 and Q_3 decouple from the other equations. We thus consider only M, N, and Q_1. In terms of these variables, and $\theta=0$, Eq. (3.8) reduces to Eq. (3.2) (with $Q_1\to Q$ and again $v_{12}\to v_{12}+2\bar{v}_{12}$). The mixed phase will thus exist only if $v_{11}v_{22}>(v_{12}+2\bar{v}_{12})^2$. If these variables are not too far from their initial values, Eq. (A10), then this condition clearly does not hold.

For $\theta=\pi/4$, Eq. (C18) yields $Q_1=Q_2$. Contrary to the situation for $\theta=0$, we may now have $Q_{12}\neq 0$. However, Eq. (C16) is not always sufficient to determine Q_{12}: For large positive r_Q, Q_{12} is very small. If one ignores Q_{12} then Eq. (3.8) again reduces to an expression very similar to Eq. (3.2), and a solution can be found, similar to that discussed in II. For smaller r_Q, Eq. (C16) yields

$$Q_{12}=-\tfrac{1}{2}(w_1M^2-w_2N^2)/r_Q\ ,$$

and this can be substituted in Eqs. (C12)–(C14), which can then be solved in a way similar to that outlined above. However, the fact that r_Q appears in the denominator indicates that some trouble will be encountered as $r_Q\to 0$. Indeed, when r_Q becomes small one must include in the Hamiltonian higher-order terms in Q_{12}, i.e., terms of quartic order (e.g., Q_{12}^4).[8] We leave such a detailed analysis for future studies.

*Present address: Baker laboratory, Cornell Univ., Ithaca, N. Y. 14853.
†Address during 1979/80: Phys. Dept. Harvard Univ, Cambridge, Mass. 02138.

[1]S. Fishman and A. Aharony, Phys. Rev. B 18, 3507 (1978). See also A. Aharony and S. Fishman, Phys. Rev. Lett. 37, 1587 (1976).
[2]S. Fishman and A. Aharony, Phys. Rev. B 19, 3776 (1979).
[3]S. F. Edwards and P. W. Anderson, J. Phys. F 5, 965 (1975).
[4]J. A. Mydosh, in *Amorphous Magnetism II*, edited by R. A. Levy and R. Hasegawa (Plenum, New York, 1977), p. 73.
[5]K. H. Fischer, Physica B+C 86, 813 (1977).
[6]K. Binder and K. Schröder, Solid State Commun. 18, 1361 (1976); Phys. Rev. B 14, 2142 (1976).
[7]S. Kirkpatrick, Proceedings of the 1978 Les Houches Summer School (unpublished).

[8]A. B. Harris, T. C. Lubensky, and J. H. Chen, Phys. Rev. Lett. 36, 415 (1976).
[9]J. H. Chen and T. C. Lubensky, Phys. Rev. B 16, 2106 (1977).
[10]A. B. Harris and T. C. Lubensky, Phys. Rev. B 16, 2141 (1977).
[11]D. C. Mattis, Phys. Lett. A 56, 421 (1976); A. Aharony and Y. Imry, Solid State Commun. 20, 899 (1976); J. M. Luttinger, Phys. Rev. Lett. 37, 778 (1976).
[12]R. Fisch and A. B. Harris, Phys. Rev. Lett. 38, 785 (1977).
[13]A. P. Young and R. B. Stinchcombe, J. Phys. C 9, 4419 (1976).
[14]C. Jayaprakash, J. Chalupa, and M. Wortis, Phys. Rev. B 15, 1495 (1977).
[15]M. Wortis, C. Jayaprakash, and E. K. Riedel, J. App. Phys. 49, 1335 (1978).
[16]A. J. Bray, M. A. Moore, and P. Reed, J. Phys. C 11, 1187 (1978); A. J. Bray and M. A. Moore, J. Phys. F 7, L333 (1977).
[17](a) D. Sherrington and S. Kirkpatrick, Phys. Rev. Lett. 35, 1792 (1975); (b) S. Kirkpatrick and D. Sherrington, Phys. Rev. B 17, 4384 (1978).
[18]D. J. Thouless, P. W. Anderson, and R. G. Palmer, Philos. Mag. 35, 593 (1977).
[19]M. W. Klein, L. J. Schowalter, and P. Shukla, Phys. Rev. B 19, 1492 (1979).
[20]J. Hubbard, Phys. Lett. 39 A, 365 (1972).
[21]For a recent review, including many references, see, e.g., A. Aharony, J. Magn. Magn. Mater. 7, 198 (1978).
[22]V. J. Emery, Phys. Rev. B 11, 239 (1975).
[23]M. Suzuki, Prog. Theor. Phys. (Japan) 58, 1151 (1977).
[24]L. D. Landau and E. M. Lifshitz, *Statistical Physics* (Pergamon, New York, 1977), Chap. XIV.
[25]K. H. Fischer, Solid State Commun. 18, 1515 (1976).
[26]J. R. L. de Almeida and D. J. Thouless, J. Phys. A 11, 983 (1978).
[27]A. J. Bray and M. A. Moore (unpublished).
[28]J. L. van Hemmen and R. G. Palmer (unpublished).
[29]D. Sherrington, J. Phys. A 11, L185 (1978).
[30]K. G. Wilson and J. Kogut, Phys. Rep. 12, 75 (1974).
[31]A. Aharony, in *Phase Transitions and Critical Phenomena,* edited by C. Domb and M. S. Green (Academic, New York, 1976), Vol. 6, p. 357.
[32](a) M. E. Fisher, Phys. Rev. Lett. 34, 1634 (1975); (b) M. E. Fisher, in *Magnetism and Magnetic Materials, San Francisco, 1974,* edited by C. D. Graham, Jr., J. J. Rhyne, and G. H. Lander, AIP Conf. Proc. No. 24 (AIP, New York, 1975), p. 273.
[33]P. Pfeuty, D. Jasnow, and M. E. Fisher, Phys. Rev. B 10, 2088 (1974).
[34]K. Adachi, K. Sato, and M. Metsuura, J. Phys. Soc. Jpn. 29, 323 (1970). See, however, E. Stryjewski and N. Gioradano, Adv. Phys. 26, 487 (1977).
[35]H. Maletta and P. Convert, Phys. Rev. Lett. 42, 108 (1979).
[36]E. Pytte and J. Rudnick, Phys. Rev. B 19, 3603 (1979); G. Grinstein (private communication).
[37]D. J. Elderfield and A. J. McKane, Phys. Rev. B 18, 3730 (1978).
[38]The required angular integrals are given in: A. Aharony and M. E. Fisher, Phys. Rev. B 8, 3323 (1973).